JOC The Journal of Organic Chemistry

Note

pubs.acs.org/joc

# Effect of Substituents on the Bond Strength of Air-Stable Dicyanomethyl Radical Thermochromes

Joshua P. Peterson, Margarita R. Geraskina, Rui Zhang, and Arthur H. Winter*

Department of Chemistry, Iowa State University, 2101d Hach Hall, Ames, Iowa 50011, United States

Supporting Information

**ABSTRACT:** A series of substituted aryl dicyanomethyl radicals were synthesized, and the bonding thermodynamic parameters for self-dimerization were determined from van't Hoff plots obtained from variable-temperature electron paramagnetic resonance and ultraviolet−visible spectroscopy. At low temperatures, the radicals dimerize, but the colored, air-stable free radicals return upon heating. Heating and cooling cycles (5−95 °C) can be repeated without radical degradation and with striking thermochromic behavior. We find a linear free energy relationship between the Hammett *para* substituent parameter and the dimerization equilibrium constant, with *para* electron-donating substituents leading to a weaker bond and electron-withdrawing substituents leading to stronger bonds, following a captodative effect. Density functional theory investigations [B98D/6-31+G(d,p)] reveal that the dimers prefer a slip-stacked geometry and feature elongated bonds.

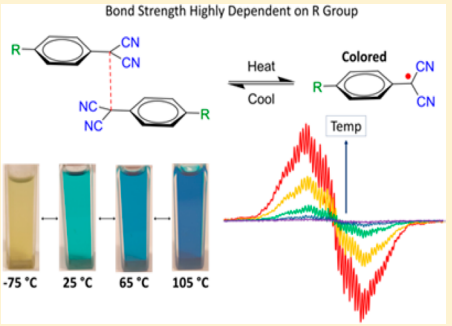


Dynamic materials that adapt their properties to environmental cues or external stimuli are increasingly being pursued. We have been interested in achieving such stimulus-responsive behavior by exploiting changes in spin state upon a stimulus because of the unique properties of radicals.[1−3] However, this approach is made challenging because many radicals lack air and thermal stability.[4−9] We were intrigued by reports of stable dicyanomethyl radicals and related radicals in the literature,[4,6,7] as well as a recent report by Kobashi et al. describing stable thermochromic triarylamino-dicyanomethyl radicals.[9] We thus set out to perform a systematic investigation of the effect of the structure of the dicyanomethyl radical on the strength of the radical bonding interaction, with an eye toward identifying potential new building blocks for stimulus-responsive materials.

A set of 11 aryl dicyanomethyl radicals were synthesized (Table 1), and the thermodynamic parameters were evaluated using van't Hoff plots generated from variable-temperature EPR and UV−vis spectroscopy experiments. The radicals were synthesized via palladium cross coupling reactions of varying aryl bromides with malononitrile, followed by oxidation to the radical using potassium ferricyanate. Remarkably, these radicals and/or radical dimers can be purified by a low-temperature biphasic separation between acetonitrile and hexane under air.

All of the radicals exhibit qualitatively the same behavior. At low temperatures, the radical dimerizes, as evidenced by a lack of an EPR signal, yielding a yellow or colorless solution. As the temperature is increased, a signal corresponding to the radical grows in the EPR and UV−vis spectrum. The radicals have absorption bands in the visible region of the optical spectrum. Example variable-temperature EPR and UV−vis data are shown in Figure 1 for radicals **1**, **3**, **4**, and **11** (all data, including a video demonstrating the thermochromic behavior, can be found in the Supporting Information). Each radical in Figure 1 has a different color, leading to striking thermochromic behavior that is highly dependent on the radical structure. To test the durability of the radical species, temperature cycling studies in which a sample was monitored for 30 min at 5 °C followed by 30 min at 95 °C were performed. After six cycles, there was no decrease in absorbance at 95 °C, confirming that the radical was thermally stable (see UV−vis insets in Figure 1).

The thermodynamic bonding parameters for all the radicals were obtained from van't Hoff plots following the growth of the EPR signal as a function of temperature and are listed in Table 1. All thermodynamic data are the average of three separate runs and fits. Inspection of the binding constants shows that better electronic donors, such as compounds **1**−**4**, have binding constants ($K_a$ = $10^5$−$10^6$ $M^{-1}$) that are lower than those of radicals bearing either weaker donating substituents or withdrawing substituents, such as compounds **5**−**10** ($K_a$ > $10^7$ $M^{-1}$).

To test if substituent effects were additive, we synthesized **11**, a trimethoxy derivative. Indeed, this radical showed the weakest dimer bond of all molecules studied ($K_a$ = 1.9 × $10^5$ $M^{-1}$), suggesting that substituent effects are additive. The compounds with less electron donation exhibit stronger binding. Compounds **5**−**8** are interesting because the halogenated derivatives **7** and **8** bind less tightly than the alkyl-substituted derivatives **5** and **6**. The ability of halogens to be both $\pi$-electron donors and $\sigma$-withdrawing groups may play a role in the weaker dimerization. Derivatives containing electron-withdrawing groups (e.g., CN and $CO_2Me$) were found to have the highest

**Received:** May 25, 2017
**Published:** May 30, 2017





DOI: 10.1021/acs.joc.7b01188
J. Org. Chem. 2017, 82, 6497−6501

**Table 1. Thermodynamic Binding Parameters and a Plot of the Log of the Binding Constant versus the Hammett $\sigma$ Parameter**

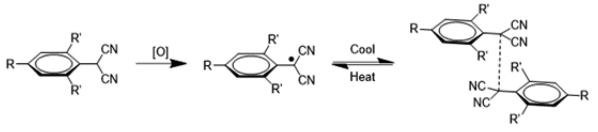


| compound | R | R′ | $\Delta H$ (kJ mol$^{-1}$) | $\Delta S$ (J mol$^{-1}$ K$^{-1}$) | $K_a$ (M$^{-1}$) |
|---|---|---|---|---|---|
| **1** | $N(CH_3)_2$ | H | −54 | −67 | $6.4 \times 10^5$ |
| **2** | S-$CH_3$ | H | −83 | −94 | $3.3 \times 10^6$ |
| **3** | O-$CH_3$ | H | −115 | −155 | $3.9 \times 10^6$ |
| **4** | *N*-morpholine | H | −82 | −142 | $8.9 \times 10^5$ |
| **5** | $CH_3$ | H | −100 | −119 | $3.2 \times 10^7$ |
| **6** | $C_6H_5$ | H | −100 | −122 | $3.9 \times 10^7$ |
| **7** | Cl | H | −103 | −150 | $9.0 \times 10^6$ |
| **8** | F | H | −104 | −129 | $1.5 \times 10^7$ |
| **9** | CN | H | −107 | −120 | $1.8 \times 10^8$ |
| **10** | $CO_2Me$ | H | −117 | −152 | $2.7 \times 10^8$ |
| **11** | O-$CH_3$ | O-$CH_3$ | −48 | −42 | $1.9 \times 10^5$ |

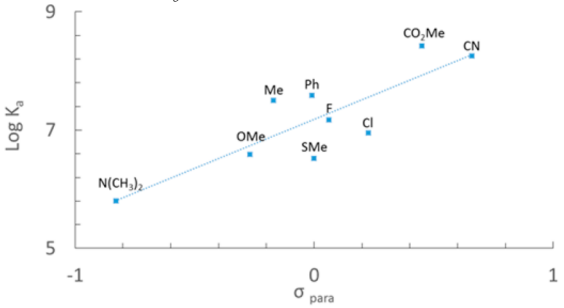


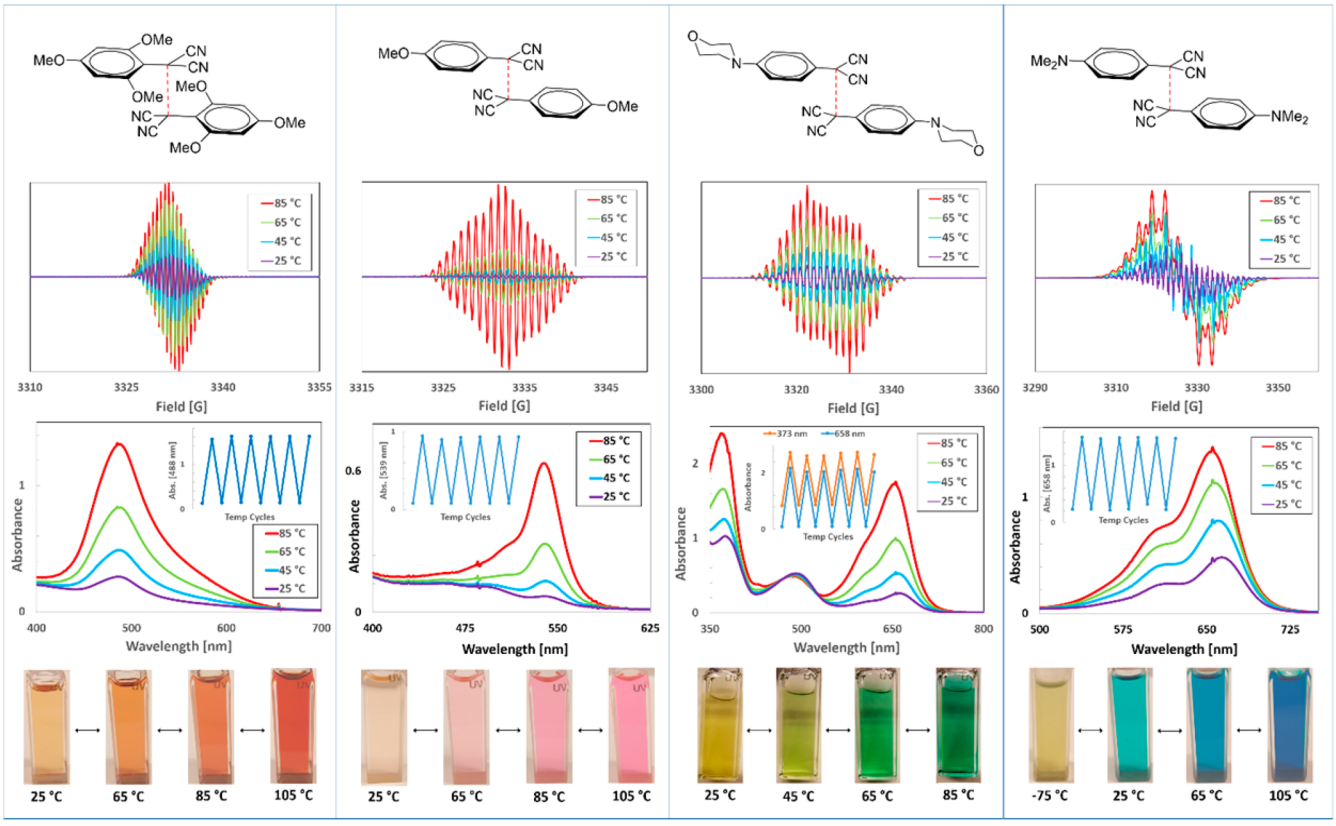


**Figure 1.** Structures of example dimer species (top row). Variable-temperature EPR study (second row). Variable-temperature UV−vis study (third row). Insets show the temperature cycling at 5 and 95 °C for 30 min each. Pictures demonstrating thermochromism open to air (bottom row). Pictures are shown to display full thermochromic behavior and may not represent all temperatures studied via EPR.



DOI: 10.1021/acs.joc.7b01188
J. Org. Chem. 2017, 82, 6497−6501

binding constants ($\sim 10^8$ $M^{-1}$) and even have resolved NMR spectra at room temperature. The other dimers exhibit NMR signals only at low temperatures because of fast exchange.

A plot of the Hammett $\sigma$ *para* parameter[10] for each monomer unit against the log of the binding constant showed a positive, relatively linear trend (Table 1). The existence of the captodative effect has been debated,[11,12] but this model predicts that radicals containing both donating and withdrawing groups would be stabilized. Given that donating substituents lead to the weakest binding (and, presumably, the most stabilized radicals), our data are consistent with the captodative model.

Computational studies were performed on select dimer species to improve our understanding of the orientation of the two units with respect to the $\sigma$ bond formed between two radicals (Figure 2).[13] Surprisingly, the dihedral angle between

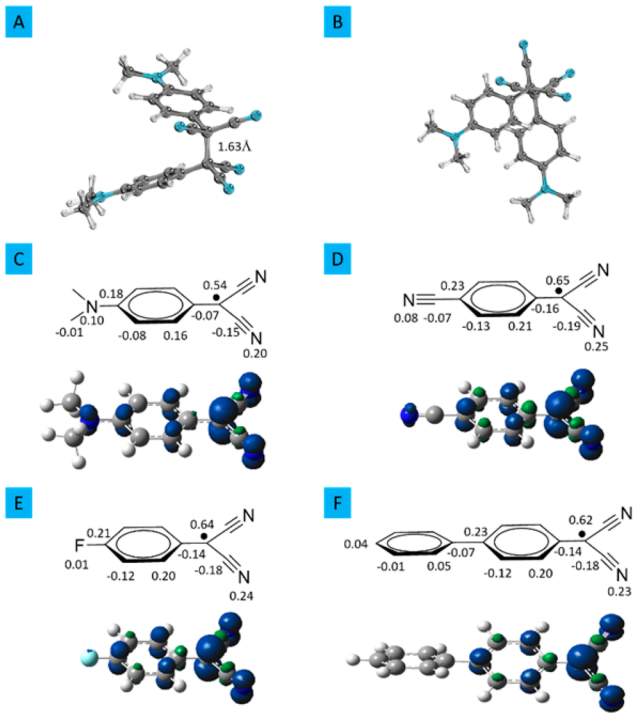


**Figure 2.** Computed structure [B98D/6-31+G(d,p)] of dimer species **1** (A, side view; B, top view). Visualized by IboView.[14,15] Computed Mulliken atomic spin densities for compounds (C) **1**, (D) **9**, (E) **8**, and (F) **6** and visualized total spin density.

the two molecules is only ~60°. Only minor variance was observed between differently substituted compounds and the calculated dihedral angle. Figure 2 shows the computed structures, at two different viewpoints, for dimer **1**, as well as the Mulliken spin densities for compounds **1**, **9**, **8**, and **6**. Each dimer features an exceptionally long computed $\sigma$ bond of ~1.63 Å.

In conclusion, we have synthesized a set of stable aryl dicyanomethyl radicals that exhibit thermochromic properties and have a bond strength that is highly dependent on the substituents. The bond strengths can be tuned from $10^5$ to $10^8$ $M^{-1}$ based on the nature of the *para* substituent. It is possible that these radicals could be incorporated into polymeric materials leading to bulk materials with temperature-responsive behavior or find use in dynamic covalent chemistries.

## EXPERIMENTAL SECTION

**General Methods.** $^1$H nuclear magnetic resonance ($^1$H NMR) and $^{13}$C nuclear magnetic resonance ($^{13}$C NMR) spectra were recorded on a Bruker DRX-500 instrument. NMR spectra were recorded in $CDCl_3$ at room temperature except where noted. The NMR data were presented accordingly: chemical shifts in parts per million with deuterated chloroform ($CDCl_3$, $\delta$ 7.26) for $^1$H NMR and the chloroform residue ($\delta$ 77.0) for $^{13}$C NMR as internal standards, multiplicity labels (s, singlet; d, doublet; t, triplet; m, multiplet), *J* splitting (hertz), and integration. EPR spectra were recorded on a Bruker FT-EPR instrument. UV−vis spectra were recorded on an Agilent 8453 spectrometer. Mass spectra were recorded on an Agilent QTOF 6540 instrument. Melting points were determined on a DigiMelt SRS apparatus. The crystal structure was obtained on a BRUKER APEX II diffractometer equipped with an APEX II CCD detector. All reactions were performed under an argon atmosphere in oven-dried glassware. Xylenes were dried under activated molecular sieves (0.4 nm). Flash column chromatography was performed with 40−63 $\mu$m silica gel (230−400 mesh) from SILICYCLE. All other chemical reagents were purchased from commercial sources and used without purification.

**General Procedure for Coupling of Malononitrile to Aryl Bromide.** To a 50 mL three-neck round-bottom flask with a magnetic stir bar was added NaOtBu (13 mmol) under an ambient atmosphere. The flask was sealed and placed under an argon atmosphere. To the flask was then added 20 mL of xylenes (dried by 0.4 nm activated molecular sieves), and the contents of the flask were stirred for 5 min to produce a uniform solution. To the flask was next added $CH_2(CN)_2$ (6.6 mmol) via syringe, and the resulting mixture was stirred for 60 min. To a separate 100 mL conical-bottom flask was added the aryl bromide of the reaction mixture (4.4 mmol) under an ambient atmosphere. The flask was pumped into a glovebox to add 0.2 g of $[Pd(PPh_3)_2]Cl_2$ catalyst (6.5 mol %). To the conical-bottom flask was then added 10−15 mL of dried xylenes, and the mixture was stirred for 5−10 min. The conical flask was cannulated into the round-bottom flask. The reaction mixture was stirred at 130 °C and the reaction monitored by TLC ($CHCl_3$ as eluent) until it reached completion. The resulting reaction was then quenched with a 10% HCl aqueous solution. The mixture was then filtered through Celite and extracted with ethyl acetate (3 × 50 mL). The organic layers were combined and dried with $Na_2SO_4$, and the solvent was removed by rotary evaporation. The crude product was then purified by flash chromatography ($CHCl_3$ as the eluent) to afford the product.

**Procedure for Oxidation of 1−11.** To a 50 mL Schlenk flask was added the aryl malononitrile (0.3 mmol) dissolved in 15 mL of $CH_2Cl_2$ along with a magnetic stir bar. The flask was flushed with argon and kept under an inert atmosphere. Separately in a 50 mL round-bottom flask was placed 15 mL of a 0.3 M KOH solution that was purged with argon. To the round-bottom flask was added $K_3[Fe(CN)_6]$ (1.5 mmol) as the oxidant. The solution was allowed to mix for 5 min before the solution was cannulated into the Schlenk flask containing the aryl malononitrile. The solution was mixed while being vigorously stirred for 10 min. The mixture was then exposed to air; the organic layer was separated and dried with $Na_2SO_4$, and the solvent was removed by rotary evaporation. The crude product was then purified by cold extraction (−78 °C) between hexanes and acetonitrile. The dimer product was kept in the solid acetonitrile, and impurities remained in the hexanes.

**EPR Studies.** All EPR studies were performed on samples purged with argon to view the hyperfine coupling of the radical species. Samples were allowed to equilibrate at each temperature for 5 min before data were acquired. The following EPR parameters were utilized for all samples unless otherwise noted: modulation frequency, 100 kHz; receiver gain, 50 dB; modulation amplitude, 0.5; time constant, 0.01 s; center field, 3300 G; sweep width, 200 G; microwave attenuation, 20 dB; microwave power, 2 mW; number of data points, 2048; average number of scans, 8. The sweep time and conversion time varied from sample to sample and are mentioned below for each compound.



DOI: 10.1021/acs.joc.7b01188
J. Org. Chem. 2017, 82, 6497−6501

**UV−Vis Studies.** To a 3 mL quartz cuvette was added a known concentration of dimer species dissolved in toluene for study. Identical results were obtained regardless of whether samples were purged with argon or under air. All samples were studied in the temperature range of 5−95 °C. A temperature-controlled water circulating bath was used to monitor the temperature, and at each data point, the sample was allowed to equilibrate to the current temperature for 5 min.

**Compound Characterization (where H denotes 1−11 and D denotes the oxidized radical dimer of that compound).** $\mathbf{1_H}$. The general procedure produced a green/yellow solid (0.383 g, 47% yield): mp 168−170 °C; $^1$H NMR (500 MHz, $CDCl_3$) $\delta$ 7.98 (d, $J$ = 7.6 Hz, 2H), 6.70 (d, $J$ = 7.6 Hz, 2H), 3.16 (s, 1H); $^{13}$C NMR (500 MHz, $CDCl_3$) $\delta$ 151.4, 128.2, 112.8, 112.6, 112.4, 40.3, 27.6. $\mathbf{1_D}$. Following the general oxidation procedure, a brilliant blue organic solution yielded a dark red solid. For EPR spectroscopy, a conversion time of 2.56 ms and a sweep time of 5.24 s were used.

$\mathbf{2_H}$. The general procedure produced a pale yellow powder (0.151 g, 20% yield): $^1$H NMR (500 MHz, $CDCl_3$) $\delta$ 7.37 (d, $J$ = 8.35 Hz, 2H), 7.30 (d, $J$ = 8.5 Hz, 2H), 5.04 (s, 1H), 2.50 (s, 3H); $^{13}$C NMR (500 MHz, $CDCl_3$) $\delta$ 142.4, 127.6, 127.0, 122.2, 111.9, 27.7, 15.2; HRMS (ESI-TOF) $m/z$ calcd for $C_{10}H_7N_2S$ 187.0335, found 187.0339 [M − H]. $\mathbf{2_D}$. Following the general oxidation procedure, a green organic solution was isolated as a yellow powder. For EPR spectroscopy, a conversion time of 2.56 ms and a sweep time of 5.24 s were used.

$\mathbf{3_H}$. The general procedure produced a pink solid (0.124 g, 15% yield): $^1$H NMR (500 MHz, $CDCl_3$) $\delta$ 7.38 (d, $J$ = 8.3 Hz, 2H), 6.97 (d, $J$ = 7.6 Hz, 2H), 5.03 (s, 1H), 3.82 (s, 3H); $^{13}$C NMR (500 MHz, $CDCl_3$) $\delta$ 160.9, 128.6, 117.9, 115.3, 112.3, 55.5, 27.4. $\mathbf{3_D}$. Following the general oxidation procedure, a pink organic solution yielded a pale yellow solid.

$\mathbf{4_H}$. The general procedure produced a beige powder (0.120 g, 12% yield): mp 153−155 °C; $^1$H NMR (500 MHz, $CDCl_3$) $\delta$ 7.34 (d, $J$ = 7.3 Hz, 2H), 6.94 (d, $J$ = 7.3 Hz, 2H), 5.00 (s, 1H), 3.84 (t, $J$ = 4.0 Hz, 4H), 3.20 (t, $J$ = 4.0 Hz, 4H); $^{13}$C NMR (500 MHz, $CDCl_3$) $\delta$ 152.5, 128.3, 116.1, 116.0, 112.3, 66.7, 48.4, 27.5; HRMS (ESI-TOF) $m/z$ calcd for $C_{13}H_{14}N_3O$ 228.1131, found 228.1136 [M + H]. $\mathbf{4_D}$. Following the general oxidation procedure, a yellow/brown organic solution yielded a brown solid. For EPR spectroscopy, a conversion time of 2.56 ms and a sweep time of 5.24 s were used. This sample used a receiver gain of 40 dB and a modulation amplitude of 1.0.

$\mathbf{5_H}$. The general procedure produced a pale yellow powder (0.570 g, 83% yield): mp 56−58 °C; $^1$H NMR (500 MHz, $CDCl_3$) $\delta$ 7.38 (d, $J$ = 8.0 Hz, 2H), 7.30 (d, $J$ = 8.0 Hz, 2H), 5.02 (s, 1H), 2.40 (s, 3H); $^{13}$C NMR (500 MHz, $CDCl_3$) $\delta$ 140.7, 130.7, 127.1, 123.2, 111.9, 27.8, 21.2. $\mathbf{5_D}$. Following the general oxidation procedure, a yellow organic solution yielded a pale yellow powder.

$\mathbf{6_H}$. The general procedure produced a white crystalline solid (0.288 g, 30% yield): mp 105−108 °C; $^1$H NMR (500 MHz, $CDCl_3$) $\delta$ 7.71 (d, $J$ = 8.3 Hz, 2H) 7.58 (m, $J$ = 8.3, 7.8 Hz, 4H), 7.49 (t, $J$ = 7.8, 7.2 Hz, 2H), 7.43 (t, $J$ = 7.2 Hz, 1H), 5.12 (s, 1H); $^{13}$C NMR (500 MHz, $CDCl_3$) $\delta$ 143.5, 139.4, 129.1, 128.7, 128.3, 127.7, 127.3, 125.0, 111.9, 27.9; HRMS (ESI-TOF) $m/z$ calcd for $C_{15}H_9N_2$ 217.0771, found 217.0776 [M − H]. $\mathbf{6_D}$. Following the general oxidation procedure, a clear organic solution yielded a white powder. For EPR spectroscopy, a modulation amplitude of 2.0, a conversion time of 2.56 ms, and a sweep time of 5.24 s were used.

$\mathbf{7_H}$. The general procedure produced a pale orange solid (0.536 g, 69% yield): mp 72−75 °C; $^1$H NMR (500 MHz, $CDCl_3$) $\delta$ 7.50 (d, $J$ = 8.7 Hz, 2H), 7.46 (d, $J$ = 8.7 Hz, 2H), 5.05 (s, 1H); $^{13}$C NMR (500 MHz, $CDCl_3$) $\delta$ 137.2, 130.7, 129.0, 125.0, 111.7, 28.0. $\mathbf{7_D}$. Following the general oxidation procedure, a yellow organic solution yielded a pale yellow powder.

$\mathbf{8_H}$. The general procedure produced a white crystalline solid (0.218 g, 31% yield): $^1$H NMR (500 MHz, $CDCl_3$) $\delta$ 7.51 (dd, $J$ = 7.0 Hz, 2H), 7.21 (t, $J$ = 7.0 Hz, 2H), 5.06 (s, 1H); $^{13}$C NMR (500 MHz, $CDCl_3$) $\delta$ 163.8, 129.4, 122.2, 117.4, 111.7, 27.6; HRMS (ESI-TOF) $m/z$ calcd for $C_9H_4FN_2$ 159.0359, found 159.0366 [M − H]. $\mathbf{8_D}$. Following the general oxidation procedure, a yellow organic solution yielded a pale yellow powder. For EPR spectroscopy, a modulation amplitude of 2.0 was used.

$\mathbf{9_H}$. The general procedure produced a slightly pink crystalline solid (0.331 g, 45% yield): mp 98−100 °C; $^1$H NMR (500 MHz, $CDCl_3$) $\delta$ 7.83 (d, $J$ = 10 Hz, 2H), 7.68 (d, $J$ = 10 Hz, 2H), 5.21 (s, 1H); $^{13}$C NMR (500 MHz, $CDCl_3$) $\delta$ 133.8, 131.1, 128.3, 117.4, 114.9, 110.9, 28.2; HRMS (ESI-TOF) $m/z$ calcd for $C_{10}H_4N_3$ 166.0411, found 166.0411 [M − H]. $\mathbf{9_D}$. Following the general oxidation procedure, a clear organic solution yielded a white powder. For EPR spectroscopy, a modulation amplitude of 2.0 was used.

$\mathbf{10_H}$. The general procedure produced a white crystalline solid (0.088 g, 10% yield): $^1$H NMR (500 MHz, $CDCl_3$) $\delta$ 8.14 (d, $J$ = 7.5 Hz, 2H), 7.59 (d, $J$ = 7.5 Hz, 2H), 5.22 (s, 1H), 3.94 (s, 3H). $\mathbf{10_D}$. Following the general oxidation procedure, a clear organic solution yielded a white powder. For EPR spectroscopy, a modulation amplitude of 2.0 was used: $^{13}$C NMR (500 MHz, $CDCl_3$) $\delta$ 165.2, 134.4, 130.9, 128.7, 128.6, 109.9, 53.0, 52.6; HRMS (ESI-TOF) $m/z$ calcd for $C_{11}H_7N_2O_2$ 199.0508, found 199.0511 [M/2].

$\mathbf{11_H}$. The general procedure produced a white crystalline solid (0.092 g, 9% yield): mp 106−108 °C; $^1$H NMR (500 MHz, $CDCl_3$) $\delta$ 6.15 (s, 2H), 5.52 (s, 1H), 3.90 (s, 6H), 3.82 (s, 3H); $^{13}$C NMR (500 MHz, $CDCl_3$) $\delta$ 163.4, 158.3, 112.5, 95.7, 91.0, 56.2, 55.6, 16.6; HRMS (ESI-TOF) $m/z$ calcd for $C_{12}H_{13}N_2O_3$ 233.0921, found 233.0919 [M + H]. $\mathbf{11_D}$. Following the general oxidation procedure, a dark red organic solution yielded an orange powder.

## ■ ASSOCIATED CONTENT

### Supporting Information

The Supporting Information is available free of charge on the ACS Publications website at DOI: 10.1021/acs.joc.7b01188.

All van't Hoff plots, variable-temperature EPR and UV−vis spectra, and computational absolute energies and Cartesian coordinates (PDF)

Crystallographic data (CIF)

A video demonstrating the thermochromic behavior examined in this work (MPG)

## ■ AUTHOR INFORMATION


### Corresponding Author

*E-mail: winter@iastate.edu.

### ORCID

Joshua P. Peterson: 0000-0002-9897-238X

Arthur H. Winter: 0000-0003-2421-5578


### Notes

The authors declare no competing financial interest.

## ■ ACKNOWLEDGMENTS

Financial support from the National Science Foundation (CHE- 1464956) and ACS PRF (PRF55820-ND4) is gratefully acknowledged. We thank Sarah Cady and the Iowa State Chemical Instrumentation Facility for assistance with the variable-temperature EPR measurements.

## ■ REFERENCES


(1) Buck, A. T.; Paletta, J. T.; Khindurangala, S. A.; Beck, C. L.; Winter, A. H. *J. Am. Chem. Soc.* **2013**, *135* (29), 10594−10597.

(2) Geraskina, M. R.; Buck, A. T.; Winter, A. H. *J. Org. Chem.* **2014**, *79* (16), 7723−7727.

(3) Juetten, M. J.; Buck, A. T.; Winter, A. H. *Chem. Commun.* **2015**, *51* (25), 5516−5519.

(4) Hartzler, H. D. *J. Org. Chem.* **1966**, *31* (8), 2654−2658.

(5) Peterson, L. I. *J. Am. Chem. Soc.* **1967**, *89* (11), 2677−2681.

(6) de Jongh, H. A. P.; de Jonge, C. R. H. I.; Sinnige, H. J. M.; de Klein, W. J.; Huysmans, W. G. B.; Mijs, W. J.; van den Hoek, W. J.; Smidt, J. *J. Org. Chem.* **1972**, *37* (12), 1960−1966.

(7) Suzuki, H.; Koide, H.; Ogawa, T. *Bull. Chem. Soc. Jpn.* **1988**, *61*, 501−504.




DOI: 10.1021/acs.joc.7b01188
*J. Org. Chem.* 2017, 82, 6497−6501

(8) de Jongh, H. A. P.; de Jonge, C. R. H. I.; Mijs, W. J. *J. Org. Chem.* **1971**, *36* (21), 3160−3168.
(9) Kobashi, T.; Sakamaki, D.; Seki, S. *Angew. Chem., Int. Ed.* **2016**, *55*, 8634.
(10) McDaniel, D. H.; Brown, H. C. *J. Org. Chem.* **1958**, *23*, 420.
(11) Leroy, G.; Dewispelaere, J. P.; Benkadour, H.; Riffi Temsamani, D.; Wilante, C. *Bull. Soc. Chim. Belg.* **1994**, *103* (7−8), 367−378.
(12) Tanaka, H. *Trends Polym. Sci.* **1993**, *1* (11), 361−365.
(13) Frisch, M. J.; Trucks, G. W.; Schlegel, H. B.; Scuseria, G. E.; Robb, M. A.; Cheeseman, J. R.; Scalmani, G.; Barone, V.; Mennucci, B.; Petersson, G. A.; Nakatsuji, H.; Caricato, M.; Li, X.; Hratchian, H. P.; Izmaylov, A. F.; Bloino, J.; Zheng, G.; Sonnenberg, J. L.; Hada, M.; Ehara, M.; Toyota, K.; Fukuda, R.; Hasegawa, J.; Ishida, M.; Nakajima, T.; Honda, Y.; Kitao, O.; Nakai, H.; Vreven, T.; Montgomery, J. A., Jr.; Peralta, J. E.; Ogliaro, F.; Bearpark, M.; Heyd, J. J.; Brothers, E.; Kudin, K. N.; Staroverov, V. N.; Kobayashi, R.; Normand, J.; Raghavachari, K.; Rendell, A. P.; Burant, J. C.; Iyengar, S. S.; Tomasi, J.; Cossi, M.; Rega, N.; Millam, N. J.; Klene, M.; Knox, J. E.; Cross, J. B.; Bakken, V.; Adamo, C.; Jaramillo, J.; Gomperts, R.; Stratmann, R. E.; Yazyev, O.; Austin, A. J.; Cammi, R.; Pomelli, C.; Ochterski, J. W.; Martin, R. L.; Morokuma, K.; Zakrzewski, V. G.; Voth, G. A.; Salvador, P.; Dannenberg, J. J.; Dapprich, S.; Daniels, A. D.; Farkas, Ö.; Foresman, J. B.; Ortiz, J. V.; Cioslowski, J.; Fox, D. J. *Gaussian 09*; Gaussian, Inc.: Wallingford, CT, 2009.
(14) Knizia, G. *J. Chem. Theory Comput.* **2013**, *9*, 4834.
(15) Knizia, G.; Klein, J. E. M. N. *Angew. Chem., Int. Ed.* **2015**, *54*, 5518−5522.



DOI: 10.1021/acs.joc.7b01188
*J. Org. Chem.* 2017, 82, 6497−6501